Electronic Supplementary Material (ESI) for RSC Advances.

Supporting Information

Construction of Bimodal Silsesquioxane-Based Porous Materials from Triphenylphosphine or Triphenylphosphine oxide and Their Size-Selective Absorption for Dye Molecules

Rong Shen[a] *and Hongzhi Liu*[a,b*]

a. Key Laboratory of Special Functional Aggregated Materials, Ministry of Education, School of Chemistry and Chemical Engineering, Shandong University, Jinan 250100, P. R. China

b. State Key Laboratory of Molecular Engineering of Polymers, Fudan University, Shanghai 200433, P. R. China

*Corresponding Author. Fax: +86 531 88364691, E-mail: liuhongzhi@sdu.edu.cn

Introduction of Three Isotherm Equations

The Langmuir model is based on the assumption that all the adsorbent sites are equivalent and there is no interaction between the adsorbate molecules formed as a monolayer. And its linear form can be written as follows:

$$\frac{1}{Q_e} = \frac{1}{Q_{\max}} + \frac{1}{K_L Q_{\max}} \times \frac{1}{C_e} \quad (1)$$

where C_e (mg L^{-1}) is the equilibrium concentration of solute, Q_e (mg g^{-1}) is the equilibrium adsorption capacity of adsorbent, Q_{max} (mg g^{-1}) is the saturated adsorption amount of adsorbent, and K_L (L g^{-1}) is the Langmuir adsorption constant.

The Freundlich model is applied to nonideal sorption on heterogeneous surfaces as well as multi-layer sorption on heterogeneous surfaces, based on the assumption that the adsorption sites are not equivalent. Its linearized equation can be expressed as follows:

$$\log Q_e = \log K_F + \frac{1}{n} \times \log C_e \quad (2)$$

where C_e (mg L^{-1}) is the equilibrium concentration of solute, Q_e (mg g^{-1}) is the equilibrium adsorption capacity of adsorbent, K_F ($mg^{1-1/n}$ $L^{1/n}$ g^{-1}) and n are Freundlich isotherm constants, which refer to the capacity and intensity of the adsorption, respectively.

Dubinin-Radushkevich model helps in determining whether an adsorption process is physical, ion exchange, or chemical type. Its linearized equation takes the form:

$$\log Q_e = \log Q_{\max} - K_D \varepsilon^2 \quad (3)$$

where K_D (mol^2 J^{-2}) is the D-R constant which is related to adsorption energy, ε is the Polanyi potential (J mol^{-1}) calculated as:

$$\varepsilon = RT \log(1 + \frac{1}{C_e}) \quad (4)$$

R is the gas constant (J mol^{-1} K^{-1}), T is the absolute temperature (K), and C_e (mg L^{-1}) is the dye concentration at equilibrium. The D-R constant is used to calculate mean free energy of adsorption E as:

$$E = \frac{1}{\sqrt{2K_D}} \quad (5)$$

The type of adsorption process can be identified by the value of E. If the value of E is <8 kJ mol^{-1}, physical adsorption prevails. If value is between 8 and 16 kJ mol^{-1}, the adsorption may be ion exchange adsorption. When E is > 16 kJ mol^{-1}, chemical adsorption may explain the adsorption type.

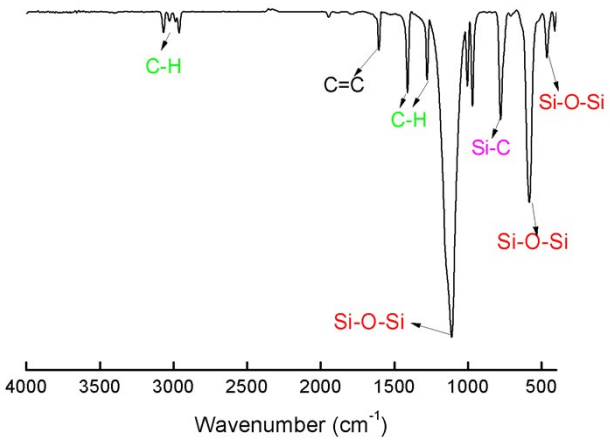

Figure S1. FTIR spectrum of OVS.

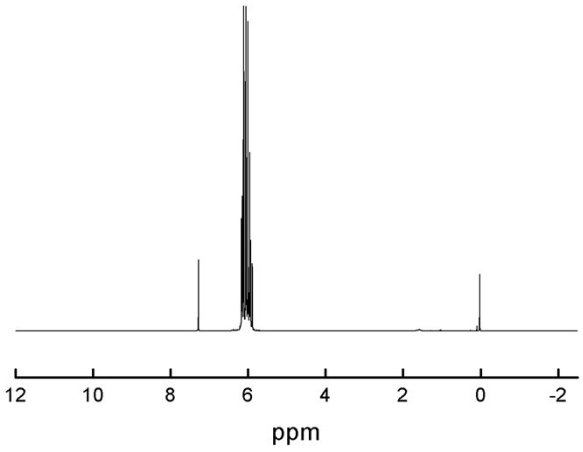

Figure S2. ^{1}H NMR spectrum of OVS.

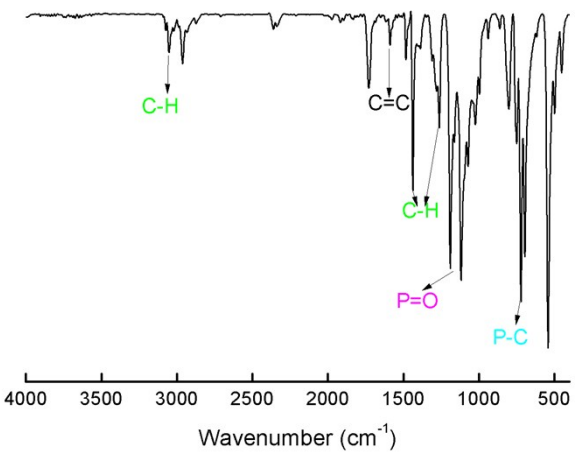

Figure S3. FTIR spectrum of TPPO.

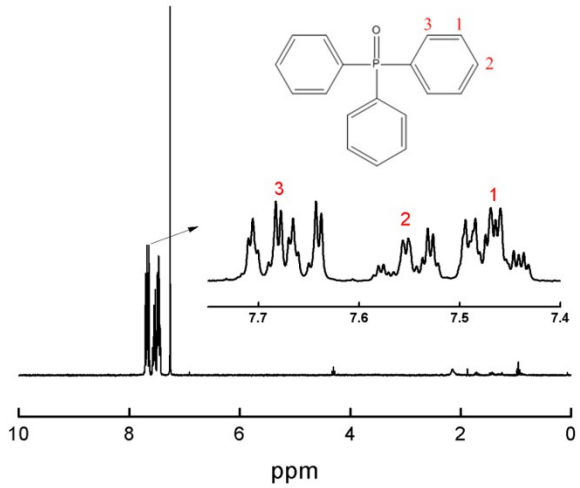

Figure S4. ^{1}H NMR spectrum of TPPO.

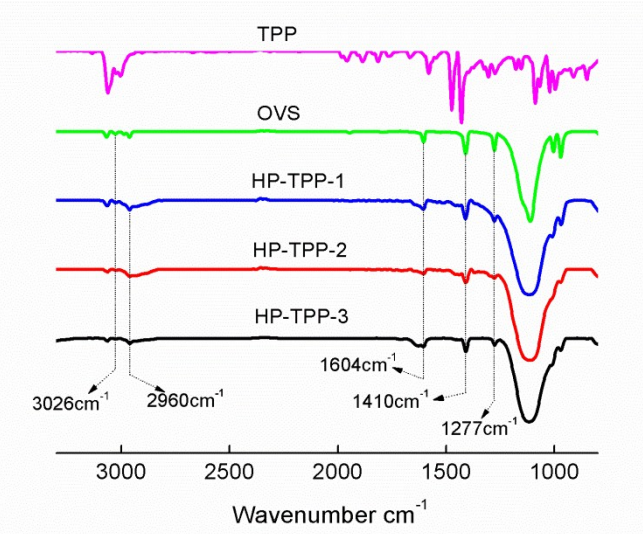

Figure S5. FTIR spectra of HP-TPPs, TPP and OVS.

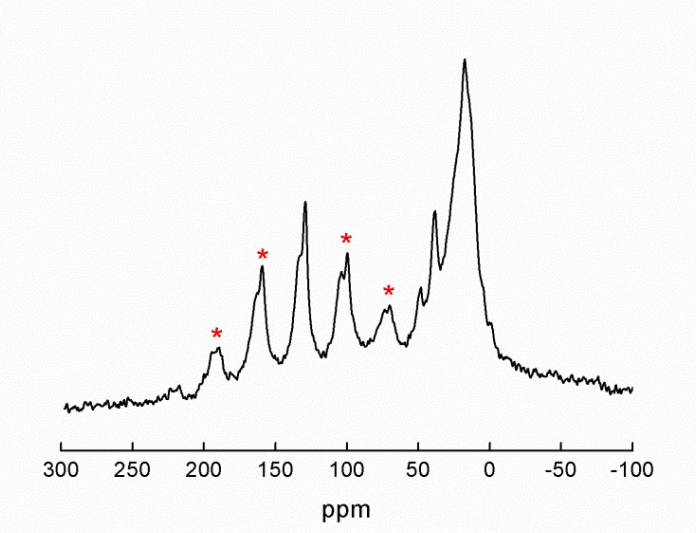

Figure S6. Solid-state ^{13}C CP/MAS NMR spectrum of HP-TPP-3('*'means satellite peaks).

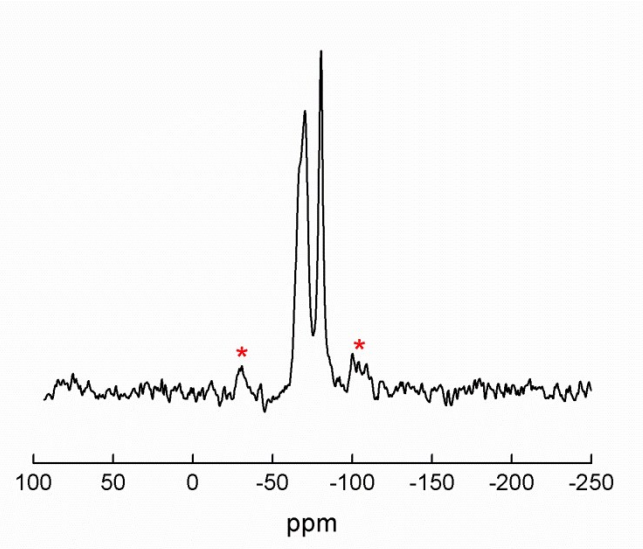

Figure S7. Solid-state ^{29}Si MAS NMR spectrum of HP-TPP-3(‘* ’means satellite peaks).

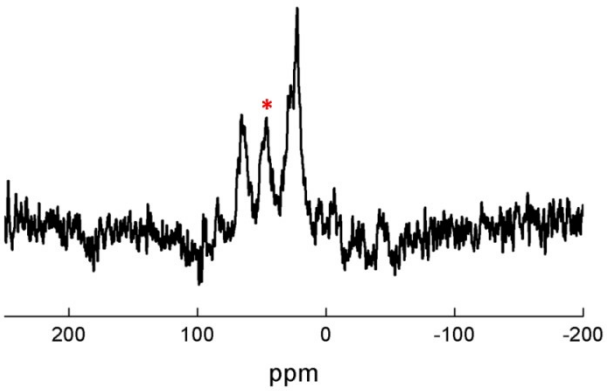

Figure S8. Solid-state ^{31}P HPDEC/MAS NMR spectrum of HP-TPP-3(‘* ’means spinning sidebands).

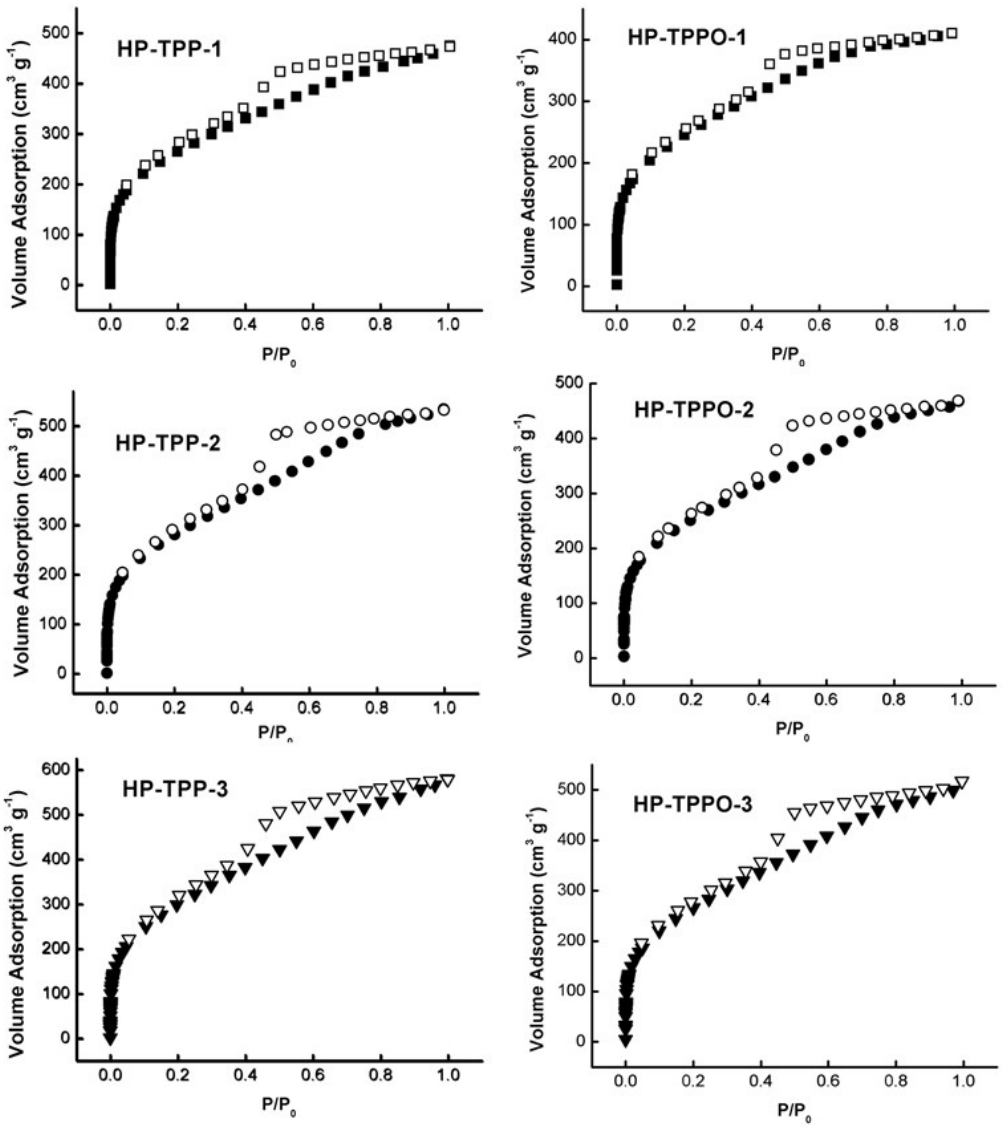

Figure S9. N_2 sorption isotherms of HP-TPPs and HP-TPPOs.

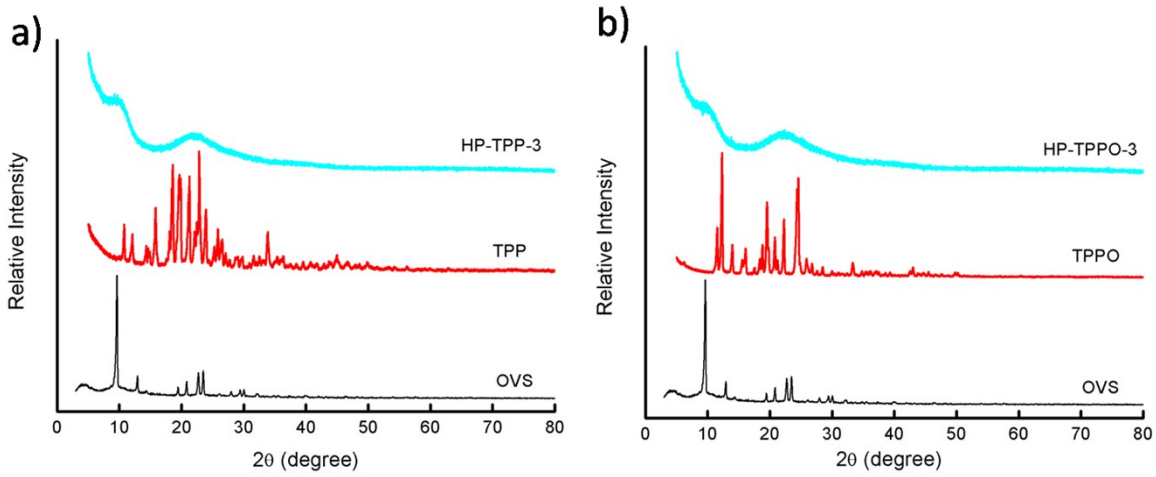

Figure S10. PXRD patterns of a)OVS, TPP and HP-TPP-3; b) OVS,

TPPO and HP-TPPO-3.

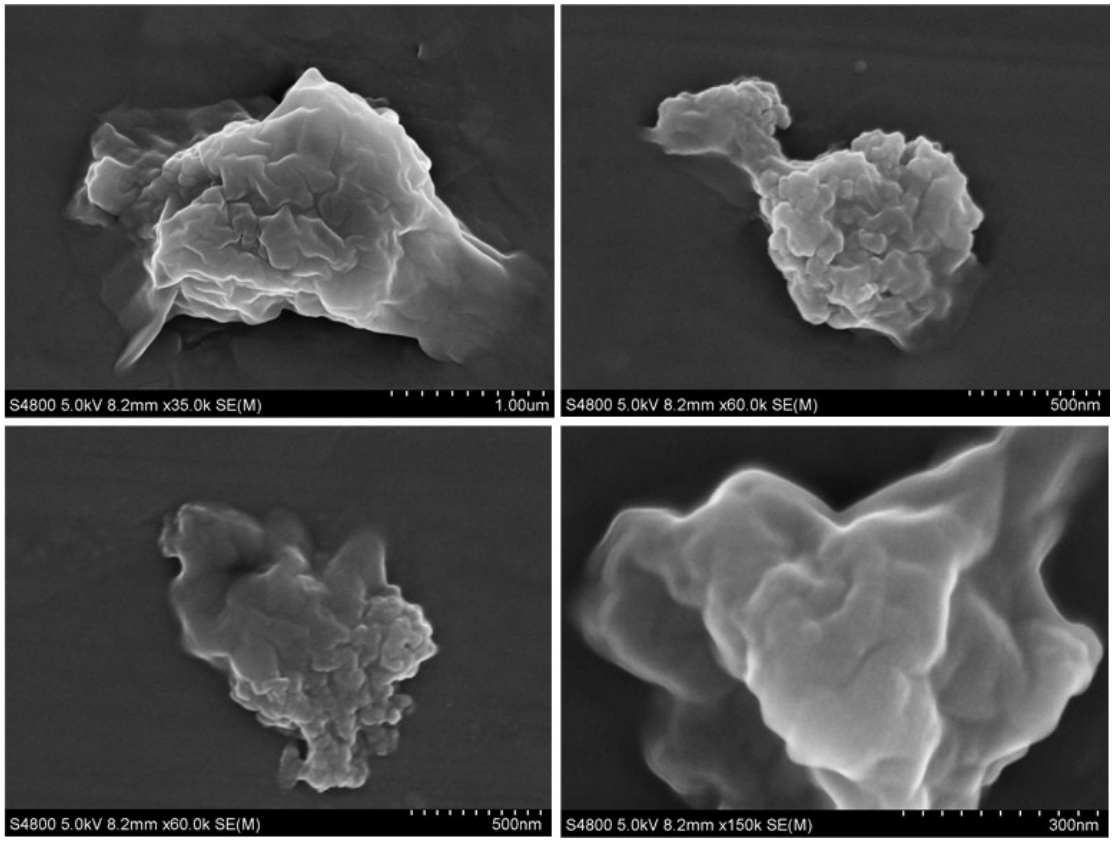

Figure S11. FE-SEM images of HP-TPPO-3.

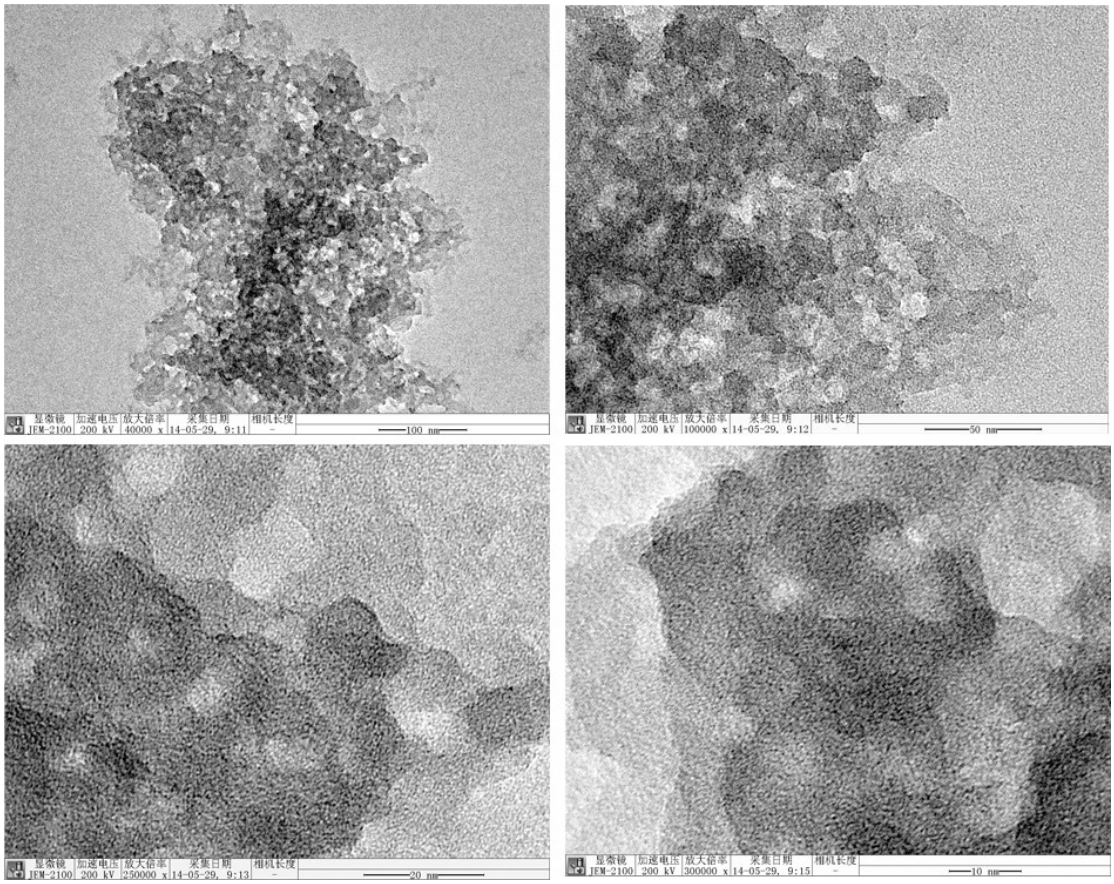

Figure S12. HR-TEM images of HP-TPPO-3.

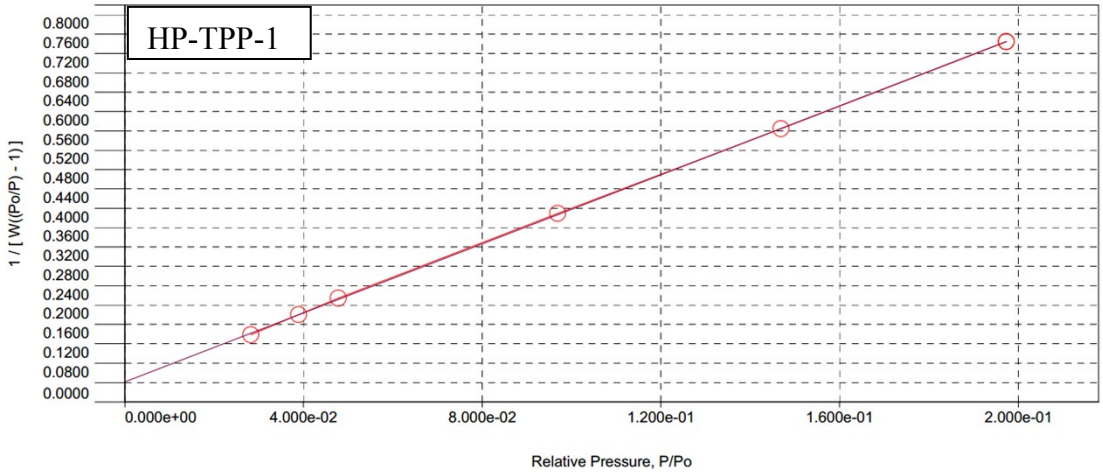

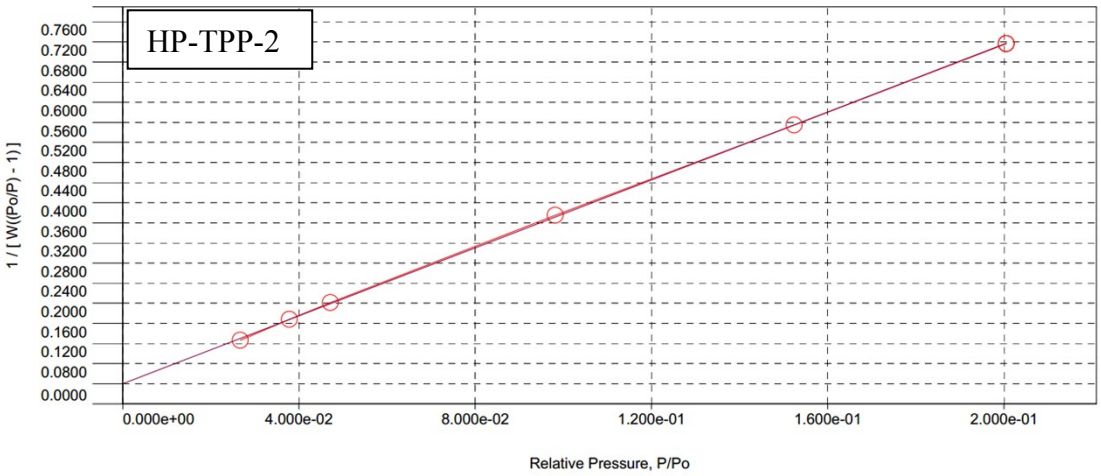
HP-TPP-2
1 / [W((Po/P) - 1)]
0.7600
0.7200
0.6800
0.6400
0.6000
0.5600
0.5200
0.4800
0.4400
0.4000
0.3600
0.3200
0.2800
0.2400
0.2000
0.1600
0.1200
0.0800
0.0000
0.000e+00
4.000e-02
8.000e-02
1.200e-01
1.600e-01
2.000e-01
Relative Pressure, P/Po

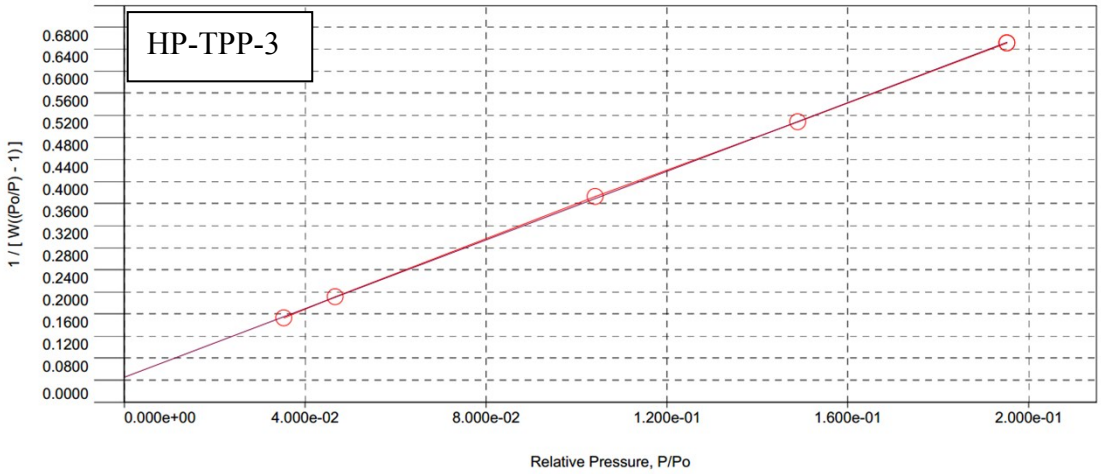
HP-TPP-3
1 / [W((Po/P) - 1)]
0.6800
0.6400
0.6000
0.5600
0.5200
0.4800
0.4400
0.4000
0.3600
0.3200
0.2800
0.2400
0.2000
0.1600
0.1200
0.0800
0.0000
0.000e+00
4.000e-02
8.000e-02
1.200e-01
1.600e-01
2.000e-01
Relative Pressure, P/Po

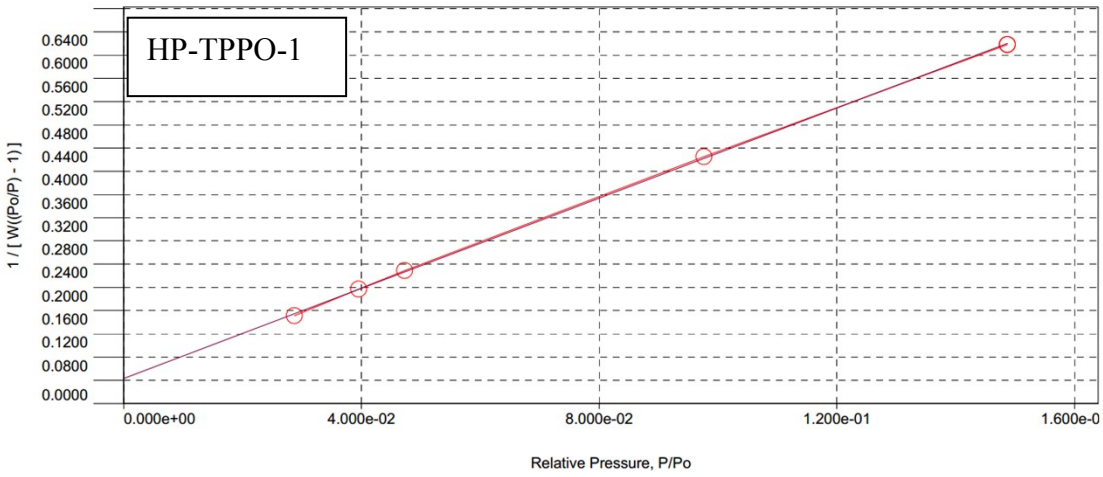
HP-TPPO-1
1 / [W((Po/P) - 1)]
0.6400
0.6000
0.5600
0.5200
0.4800
0.4400
0.4000
0.3600
0.3200
0.2800
0.2400
0.2000
0.1600
0.1200
0.0800
0.0000
0.000e+00
4.000e-02
8.000e-02
1.200e-01
1.600e-0
Relative Pressure, P/Po

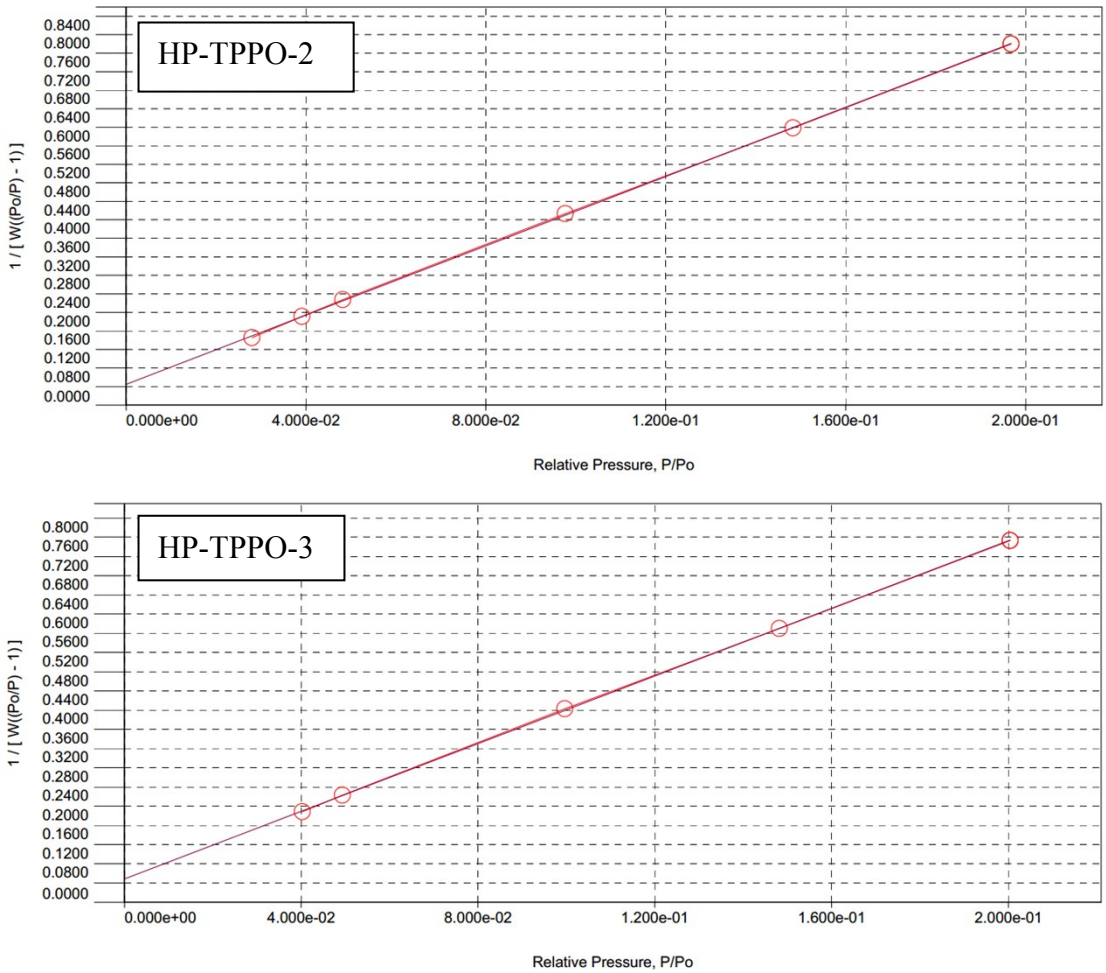

Figure S13. BET plots of HP-TPP-1(r=0.999961, C=86.838), HP-TPP-2(r=0.999944, C=86.092), HP-TPP-3(r=0.999940, C=69.654), HP-TPPO-1(r=0.999909, C=91.258), HP-TPPO-2(r=0.999946, C=84.969) and HP-TPPO-3(r=0.999966, C=73.426).

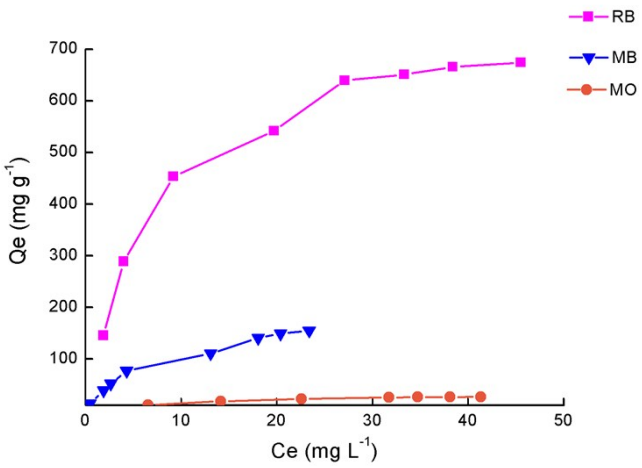

Figure S14. Adsorption isotherms for rhodamine B (RB), methylene blue (MB), and methyl orange (MO) onto HP-TPP-3.

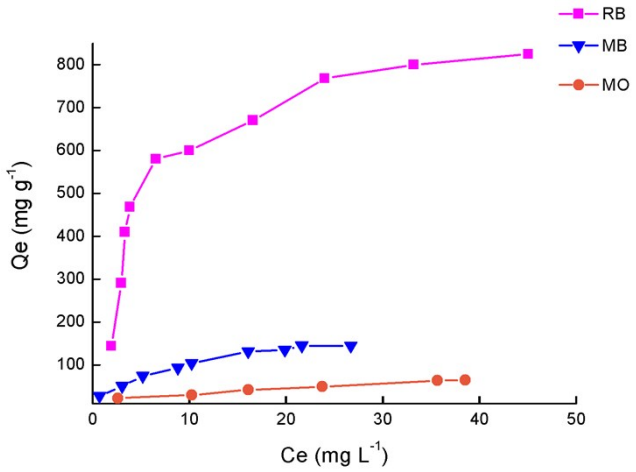

Figure S15. Adsorption isotherms for rhodamine B (RB), methylene blue (MB), and methyl orange (MO) onto HP-TPPO-3.

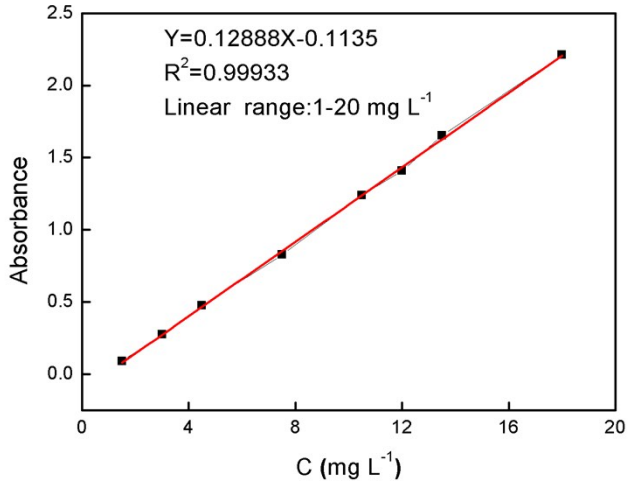

Figure S16. The low-limit of detection with a linear fit in the linear concentration range of methylene blue (MB).

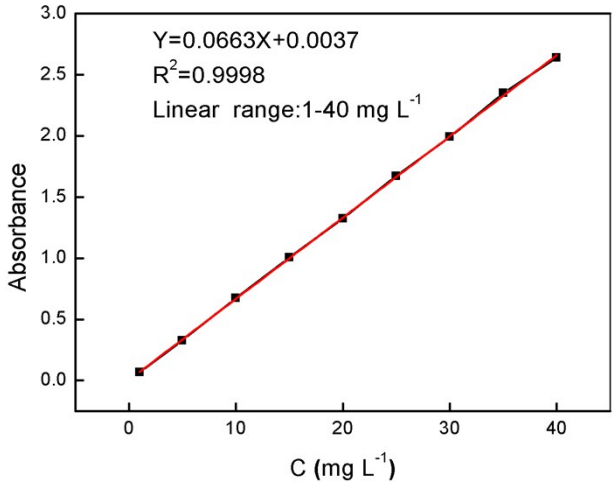

Figure S17. The low-limit of detection with a linear fit in the linear concentration range of methyl orange (MO).

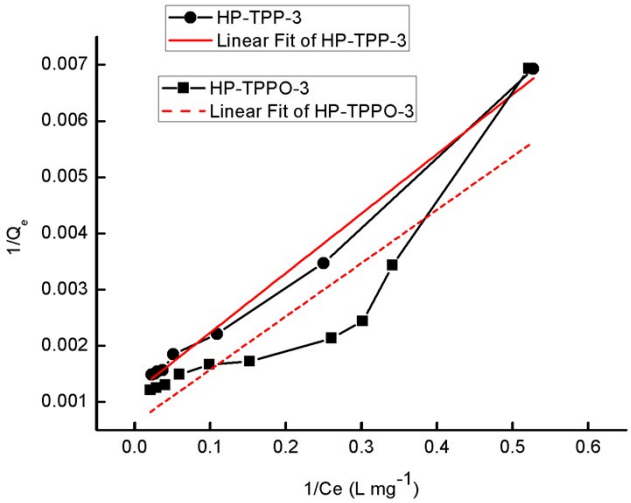

Figure S18. Langmuir isotherm model for rhodamine B onto HP-TPP-3 and HP-TPPO-3.

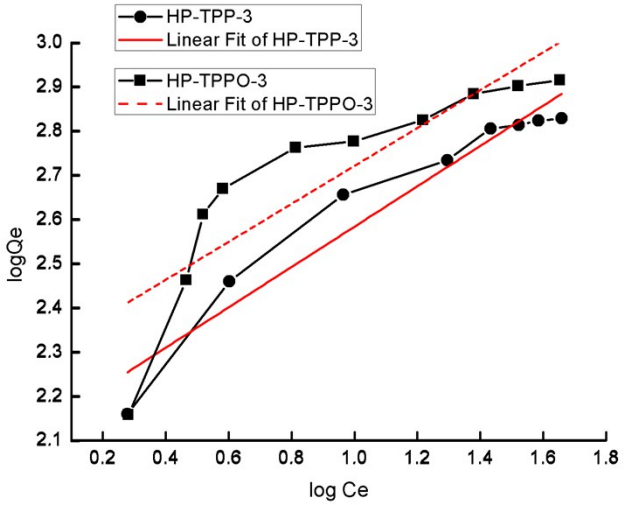

Figure S19 Freundlich isotherm model for rhodamine B onto HP-TPP-3 and HP-TPPO-3.

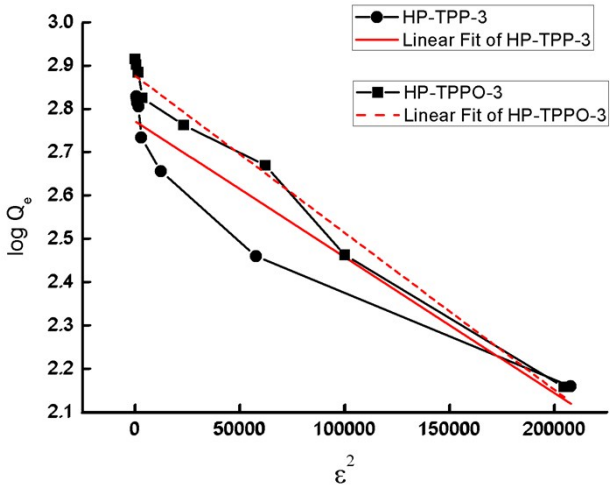

Figure S20. Dubinin-Radushkevich isotherm model for rhodamine B onto HP-TPP-3 and HP-TPPO-3.

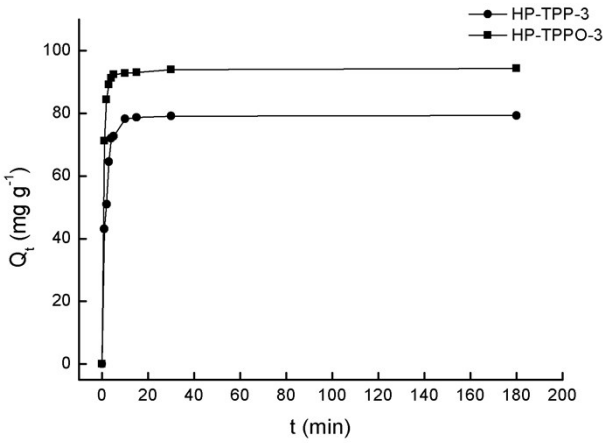

Figure S21. Adsorption kinetics curves for the adsorption of rhodamine B with initial concentration of 50.0 ppm onto HP-TPP-3 and HP-TPPO-3.

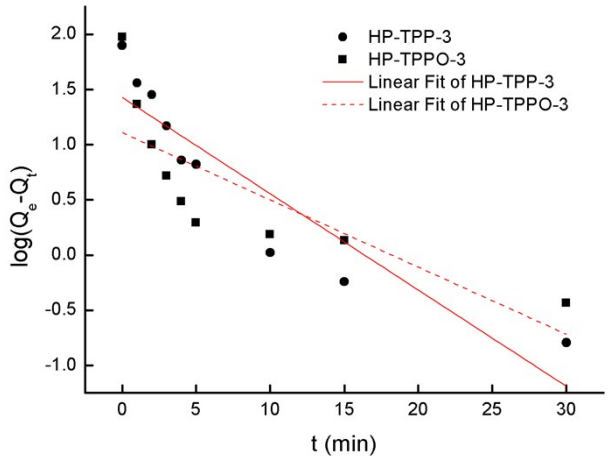

Figure S22. Pseudo-first-order kinetics for the adsorption of rhodamine B with initial concentration of 50.0 ppm onto HP-TPP-3 and HP-TPPO-3.

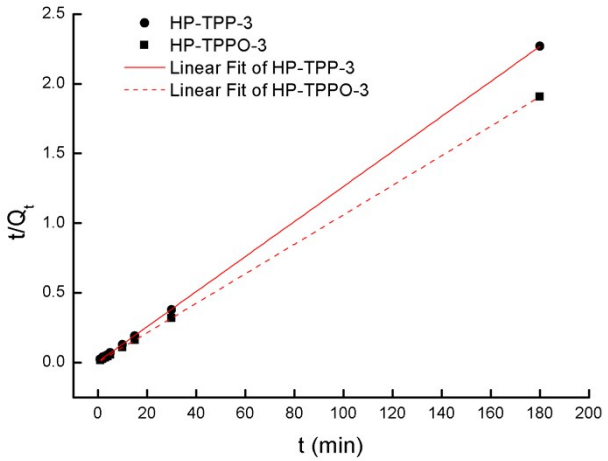

Figure S23. Pseudo-second-order kinetics for the adsorption of rhodamine B with initial concentration of 50.0 ppm onto HP-TPP-3 and HP-TPPO-3.

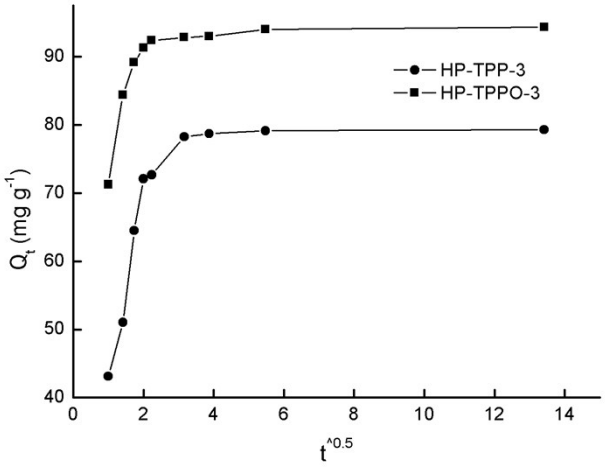

Figure S24. Intraparticle diffusion kinetics for the adsorption of rhodamine B with initial concentration of 50.0 ppm onto HP-TPP-3 and HP-TPPO-3.

Table S1. Elemental analysis of HP-TPPs and HP-TPPOs.

Sample	Experimental Value		Theoretical Value	
	C%	H%	C%	H%
HP-TPP-1	32.85	5.16	44.39	4.35
HP-TPP-2	36.83	4.50	41.64	4.24
HP-TPP-3	28.38	4.04	39.79	4.17
HP-TPPO-1	36.78	4.30	43.67	4.28
HP-TPPO-2	33.04	4.13	41.09	4.19
HP-TPPO-3	32.67	4.07	39.35	4.13

Table S2. Comparison of adsorbents for removal of rhodamine B.

Materials	Preparation method	Physical parameters	Adsorption capacity (mg g^{-1})	References
HP-TPP-3	Friedel-Crafts reaction	S_{BET}: 1105 m^2 g^{-1}	674.6	This work
HP-TPPO-3	Friedel-Crafts reaction	S_{BET}: 976 m^2 g^{-1}	828.6	This work
Fe3O4@POSS-SH	Polymerization and Thiol-ene addition reaction for postfunctionalization	S_{BET}: 224.20 m^2 g^{-1}	142.05	1
Magnetic mesoporous silica	Sol-gel method and oxidation at high temperature	S_{BET}: 842.75 m^2 g^{-1}	105.04	2
SO_3H-HSM	sol–gel method and modified with sulfonic groups	S_{BET}: 345.69 m^2 g^{-1}	271.00	3
MPSC/C	surfactant-templating approach	S_{BET}: 2580 m^2 g^{-1}	785	4

References

1. H. B. He, B. Li, J. P. Dong, Y. Y. Lei, T. L. Wang, Q. W. Yu, Y. Q. Feng and Y. B. Sun, *ACS Appl Mater Interfaces,* 2013, **5**, 8058-66.
2. S. Tao, Z. Zhu, C. Meng and C. Wang, *Microporous Mesoporous Mater.,* 2013, **171**, 94-102.
3. W. Shi, S.Tao, Y. Yu, Y. Wang and W. Ma, *J. Mater. Chem.,* 2011, **21**, 15567-15574.
4. X. Zhuang, Y. Wan, C. Feng, Y. Shen and D. Zhao, *Chem. Mater.,* 2009, **21**, 706-716.